engineering proceedings

MDPI

Proceeding Paper

Optical and Mechanical Characterization of Lignocaine-Impregnated Maltose-Based Dissolvable Microneedles †

Arifah Syahirah Rahman [1], Fook-Choe Cheah [2], Mohd Eusoff Azizol Nashriby [1], Mae-Lynn Catherine Bastion [2], Chang Fu Dee [1], Muhamad Ramdzan Buyong [1], Mohd Ambri Mohamed [1], Xin Yun Chua [3], Poh Choon Ooi [1], Muhammad Irfan Abdul Jalal [4], Chenshen Lam [2], Yin Yen Mun [2], Chee Seong Goh [5], Ahmad Ghadafi Ismail [1,*] and Azrul Azlan Hamzah [1,*]

[1] Institute of Microengineering and Nanoelectronics (IMEN), Level 4, Research Complex, Universiti Kebangsaan Malaysia (UKM), Bangi 43600, Selangor, Malaysia; arifahrahman@ukm.edu.my (A.S.R.); p145465@siswa.ukm.edu.my (M.E.A.N.); cfdee@ukm.edu.my (C.F.D.); muhdramdzan@ukm.edu.my (M.R.B.); ambri@ukm.edu.my (M.A.M.); pcooi@ukm.edu.my (P.C.O.)

[2] Department of Ophthalmology, Hospital Cancelor Tuanku Muhriz, Faculty of Medicine, Universiti Kebangsaan Malaysia (UKM), Jalan Yaacob Latif, Bandar Tun Razak, Cheras 56000, Kuala Lumpur, Malaysia; cheahfc@hctm.ukm.edu.my (F.-C.C.); mae-lynn@hctm.ukm.edu.my (M.-L.C.B.); chenshen_lam@yahoo.com (C.L.); charlotte_myy@hotmail.com (Y.Y.M.)

[3] Jabatan Farmasi, Hospital Canselor Tuanku Muhriz (HCTM), Universiti Kebangsaan Malaysia (UKM), Jalan Yaacob Latif, Bandar Tun Razak, Cheras 56000, Kuala Lumpur, Malaysia; chuaxinyun@hctm.ukm.edu.my

[4] UKM Medical Molecular Biology Institute, Hospital Canselor Tuanku Muhriz (HCTM), Universiti Kebangsaan Malaysia (UKM), Jalan Yaacob, Latif, Bandar Tun Razak, Cheras 56000, Kuala Lumpur, Malaysia; irfan.abduljalal@ukm.edu.my

[5] Alnair Photonics Sdn Bhd, 13, Persiaran Mahsuri 1/1, Sunway Tunas, Bayan Lepas 11900, Pulau Pinang, Malaysia; goh@alnair-labs.com

* Correspondence: ghad@ukm.edu.my (A.G.I.); azlanhamzah@ukm.edu.my (A.A.H.); Tel.: +60-3-8911-8545 (A.G.I.); +60-3-8911-8020 (A.A.H.)

† Presented at the 2nd International Conference on AI Sensors and Transducers, Kuala Lumpur, Malaysia, 29 July–3 August 2025.

Abstract

Dissolvable microneedles (DMNs) represent an innovative approach to patient-friendly drug delivery, eliminating the need for conventional hypodermic injections. This study reports on the fabrication, Confocal Laser Scanning Microscopy (CLSM)-based optical visualization of drug distribution, and mechanical characterization of maltose-based DMNs impregnated with lignocaine, a local anesthetic. Microneedles were fabricated using a micro-molding technique and dried for nine hours. Structural integrity was evaluated using Field Emission Scanning Electron Microscopy (FESEM); drug distribution was examined via CLSM; and mechanical strength was assessed using nanoindentation. The FESEM results showed uniform microneedle formation with sharp tips and smooth surfaces, averaging 435 µm in height and 116 µm in width, with no significant dimensional variability ($p > 0.5$). CLSM analysis indicated even distribution of lignocaine throughout the matrix. Mechanical testing showed that each microneedle withstood 0.6 N, surpassing the 0.1 N threshold required for skin insertion. These results support the viability of maltose-based DMNs for local anesthetic delivery, with implications for outpatient, pediatric, and self-administered care settings. Future investigations will include Franz diffusion and in vitro dissolution studies to examine release kinetics.

Keywords: dissolvable microneedles; lignocaine; maltose; FESEM; CLSM; nanoindentation

check for updates

Academic Editor: Sang-Seok Lee

Published: 14 January 2026

Citation: Rahman, A.S.; Cheah, F.-C.; Nashriby, M.E.A.; Bastion, M.-L.C.; Dee, C.F.; Buyong, M.R.; Mohamed, M.A.; Chua, X.Y.; Ooi, P.C.; Abdul Jalal, M.I.; et al. Optical and Mechanical Characterization of Lignocaine-Impregnated Maltose-Based Dissolvable Microneedles. *Eng. Proc.* **2025**, *110*, 7. https://doi.org/10.3390/engproc2025110007

Copyright: © 2026 by the authors. Licensee MDPI, Basel, Switzerland. This article is an open access article distributed under the terms and conditions of the Creative Commons Attribution (CC BY) license (https://creativecommons.org/licenses/by/4.0/).

1. Introduction

Microneedle (MN) technology presents a viable alternative to conventional transdermal and injectable drug delivery methods [1]. Initially fabricated from rigid silicon materials, microneedles have evolved into more advanced platforms, including dissolvable, hydrogel-forming, and 3D-printed designs [2]. These innovations offer key advantages such as painless administration, faster onset of action, and the elimination of sharps waste, making them particularly suitable for outpatient and self-administered treatments [3].

Lignocaine is a commonly used local anesthetic, recognized for its rapid onset and favorable safety profile [4]. Incorporating lignocaine into dissolving microneedle systems may improve its delivery for dermatological and minor surgical procedures. However, several challenges remain. A primary concern is inconsistent drug loading within the microneedles, which can result in variable dosing [5]. Furthermore, there is a lack of standardized, non-destructive methods to verify drug distribution throughout the microneedle matrix [6].

This study focuses on the fabrication of maltose-based dissolving microneedles (DMNs) loaded with lignocaine and characterizes their morphology, drug distribution, and mechanical properties. Drug distribution (via confocal laser scanning microscopy) and mechanical testing were used to evaluate structural integrity, drug dispersion, and overall performance of the microneedles for potential clinical use.

Conventional dissolvable microneedle systems commonly encounter three limitations: uneven drug distribution, absence of direct optical confirmation, and reliance on multi-step fabrication involving costly materials or separate support layers. This study introduces a simplified, single-step method that employs maltose as both the structural and drug-carrying component, eliminating the need for backing films. Confocal microscopy was used to directly assess drug distribution within the matrix, addressing a gap often overlooked in earlier work. The integration of material efficiency, streamlined fabrication, and direct imaging defines the novelty of this approach.

2. Material and Methods

2.1. Material

Analytical-grade Maltose Monohydrate (≥99% purity;) (CAS No. 6363-53-7; R&M Chemicals, Petaling Jaya, Malaysia) was chosen as the polymer matrix for its biocompatibility and dissolvable nature. Lignocaine (CAS No. 137-58-6; MedChemExpress, Monmouth Junction, NJ, USA) served as the model anesthetic and was stored at 4 °C in sealed, dry, and light-protected conditions. Rhodamine B (Grade: GR, CAS: 81-88-9; Nacalai Tesque Inc., Kyoto, Japan) was added in trace amounts to selected formulations as a fluorescent tracer for imaging. Deionized water was used in all preparation steps to maintain consistency and matrix purity. Silicone micromolds enabled the formation of microneedle arrays with uniform dimensions and sharp tips suitable for skin penetration. All additional reagents and solvents were of analytical grade and used without further purification.

2.2. Methods

2.2.1. Fabrication Process

Dissolving microneedles (DMNs) were prepared using a single-step micro-molding technique (Figure 1). Similar to microelectromechanical systems (MEMSs), where precise etching and sacrificial layer techniques are employed for microchannel formation [7], the micromolding approach in this study ensures dimensional reproducibility critical to drug-delivery microneedles. The formulation combined maltose (analytical grade, ≥99% purity) as the structural matrix with lignocaine as the active ingredient. Lignocaine was added at

10% *w*/*w* relative to the total solids. In selected batches, a trace amount of rhodamine B was included to enable fluorescence imaging.

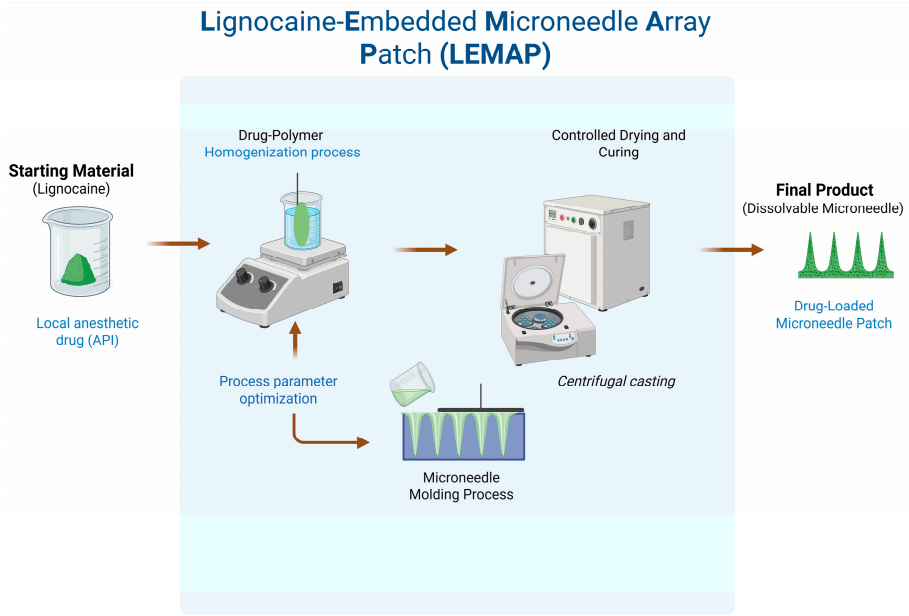

Figure 1. Conceptual workflow illustrating the preparation of lignocaine-embedded microneedle array patches (LE-MAPs).

The mixture was prepared by dissolving the components in deionized water to form a viscous solution, which was then cast into silicone micromolds. Centrifugation at 4000 rpm for 40 min ensured complete mold filling and removal of air bubbles. The maltose matrix served as both structural and backing material.

After molding, the samples were dried in a convection oven (Model:BOV-T30C; Biobase Bioland Co., Ltd., Jinan, China) at 40 °C for nine hours under atmospheric pressure. The hardened microneedle patches were then demolded and stored in sealed containers to prevent moisture exposure. The fabrication process targeted a fill efficiency of at least 90% to ensure uniform needle formation across each array.

2.2.2. Optical Characterization

Field Emission Scanning Electron Microscopy (FESEM)

Field Emission Scanning Electron Microscopy (FE-SEM) was conducted using ZEISS MERLIN Compact system controlled by ZEISS SmartSEM software (version 6.0, Carl Zeiss Microscopy GmbH, Jena, Germany), which offers resolution up to 0.8 nm at 15 kV and 30 kV in STEM mode, and 1.6 nm at 1 kV, with magnification ranging from 12× to 2,000,000×. Fe-SEM images were analyzed to evaluate microneedle geometry, including tip sharpness, surface uniformity, and dimensional consistency—parameters critical for effective skin penetration and drug delivery. Three samples, processed under identical centrifugation conditions, were each imaged at five separate locations to evaluate morphological uniformity.

Confocal Laser Scanning Microscopy (CLSM)

Confocal Laser Scanning Microscopy (CLSM) was carried out using the Leica TCS SP5 II system (Leica Microsystems GmbH, Wetzlar, Germany) to assess lignocaine distribution within the microneedle matrix. A rhodamine-labeled formulation was prepared by incorporating a small amount of rhodamine B into the maltose matrix during casting. Imaging was conducted at an excitation range of 543–561 nm and an emission range of

approximately 565–600 nm. Three microneedle samples from the same batch were examined, with fluorescence images taken at three different positions on each sample. Control patches containing only maltose, without lignocaine, were prepared and imaged under the same conditions to evaluate autofluorescence. A consistent fluorescence signal across the microneedles indicated uniform drug dispersion within the polymer matrix.

2.2.3. Mechanical Characterization

Nanoindentation was performed using a Micro Materials NanoTest™ system (Micro Materials Ltd, Wrexham, United Kingdom) fitted with a Berkovich diamond tip. Mechanical properties such as Young's modulus and hardness were calculated from load–depth data using the method described previously by Oliver and Pharr [8]. Three microneedle samples from the same batch were tested, with three indentations applied at different points on each sample. A minimum insertion force of 0.1 N was required to confirm suitability for skin penetration.

3. Results and Discussion

3.1. Field Emission Scanning Electron Microscopy (FE-SEM)

Microneedles fabricated from maltose demonstrated consistent morphology and mechanical integrity, confirming the feasibility of this platform for lignocaine delivery [9].

Figure 2 presents SEM images of maltose-based microneedles loaded with lignocaine, highlighting both vertical height and base width measurements. Panel (a) demonstrates the vertical height of representative microneedles (H1 = 418.5 µm, H2 = 423.1 µm, H3 = 413.9 µm), confirming consistent fabrication with an average tip height of ~415 µm. Panel (b) presents base width measurements (V1 = 189.4 µm, V2 = 178.7 µm), indicating consistent geometry across the microneedle array. These values confirm both the reproducibility of the micromolding method and the dimensional stability of the fabricated structures.

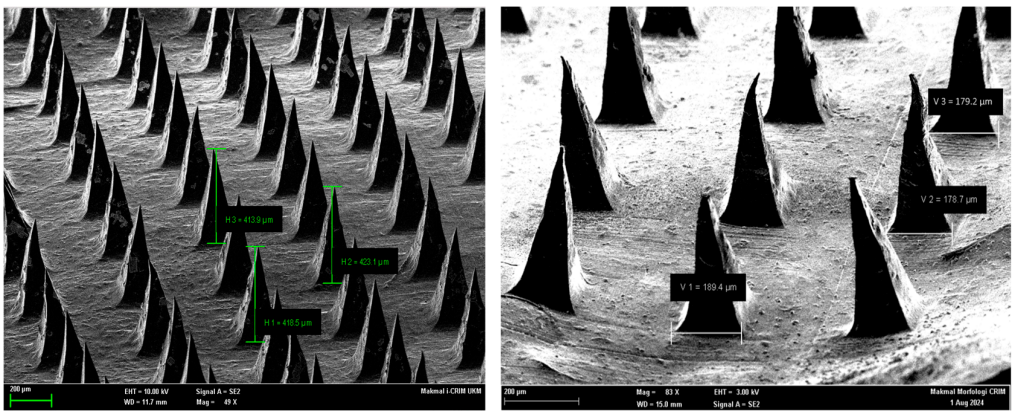

(**a**) (**b**)

Figure 2. Scanning Electron Microscopy (SEM) Images of Maltose-Based Lignocaine Microneedles Showing Tip Heights and Base Widths. Representative SEM images of maltose microneedle arrays demonstrating uniform geometry and sharp tips. (**a**) Vertical height measurements of selected microneedles (H1 = 418.5 µm, H2 = 423.1 µm, H3 = 413.9 µm) confirm consistent fabrication with tip heights averaging ~415 µm. (**b**) Base width measurements (V1 = 189.4 µm, V2 = 178.7 µm) indicate well-defined structural integrity, supporting mechanical robustness during skin penetration.

SEM imaging showed that the microneedles had sharp, well-defined tips and smooth surfaces, features necessary for efficient skin penetration. Precision at the microscale, particularly in tip geometry, is essential for effective biological interaction—a requirement reflected in the observed structures [10]. Dimensional analysis reported an average height of 435 µm and width of 116 µm, with no significant variation ($p = 0.523$ and $p = 0.601$). These

results indicate high fabrication accuracy and reproducibility, supporting the potential for clinical use.

Consistent microneedle dimensions are essential to ensure uniform skin penetration and reliable drug delivery across the patch. Structural uniformity also reduces the likelihood of partial insertion, which may result in incomplete dosing or inconsistent absorption. The sharp and smooth surfaces observed under SEM support the potential for pain-free application and effective transdermal transport. These results are consistent with earlier reports indicating that tip sharpness and geometric uniformity are key determinants of mechanical strength and successful insertion [11].

Combined with the mechanical data and drug distribution findings, the SEM results reinforce that maltose–lignocaine microneedles meet the dimensional precision, reproducibility, and robustness required for clinical translation [12].

3.2. Confocal Laser Scanning Microscopy (CLSM)

CLSM imaging provided qualitative confirmation of lignocaine distribution. Strong, uniform fluorescence was observed throughout the drug-loaded microneedles, while no signal appeared in the control patches [13]. Although drug content uniformity is a critical factor for effective microneedle-based delivery, internal drug distribution is rarely validated optically in current studies. Most reports rely on bulk quantification methods or assume homogeneity based on fabrication steps, leaving a gap in confirming spatial drug localization within the microneedle matrix [14]. This study addresses that gap by targeting a drug loading uniformity of $\geq$85%, supported by confocal imaging as a direct optical validation method. These findings confirm that the drug is present and uniformly distributed, ensuring consistent dosing and predictable therapeutic onset.

Figure 3 presents fluorescence and pseudo-colored microscopy images showing lignocaine distribution within maltose-based microneedles. In panel (a), control microneedles display minimal fluorescence, confirming the absence of lignocaine. In contrast, drug-loaded microneedles show distinct and strong fluorescence along the shafts, indicating successful incorporation of lignocaine into the matrix. This contrast confirms that the observed signal originates from the drug and not from background polymer autofluorescence.

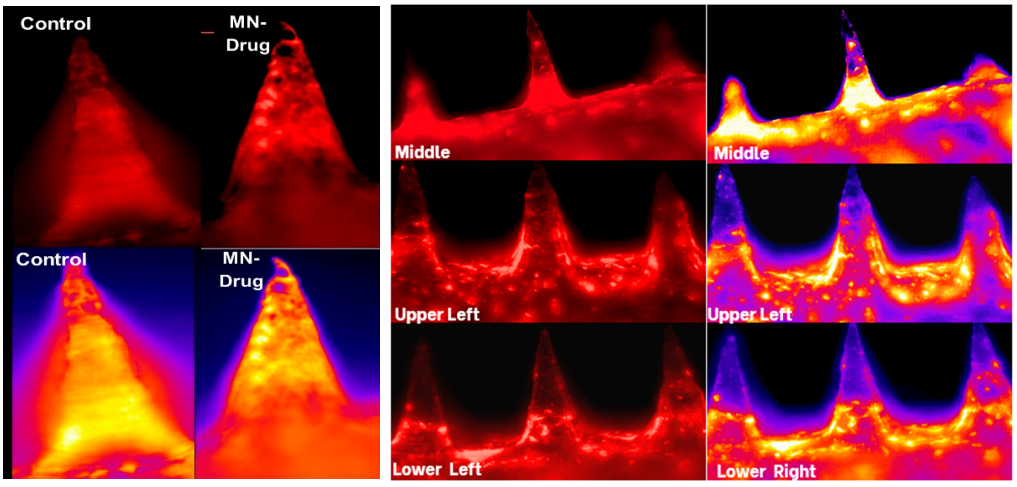

(**a**) (**b**)

Figure 3. Fluorescence microscopy images of maltose-based microneedles illustrate lignocaine distribution. (**a**) Control microneedles without lignocaine show no fluorescence, while drug-loaded microneedles display distinct fluorescence signals in pseudo-colored images, confirming drug presence; (**b**) Images taken from various positions on the patch (middle, upper left, and lateral areas) demonstrate uniform lignocaine distribution throughout the array.

Panel (b) shows fluorescence images captured at various positions across the microneedle patch (middle, upper left, and lateral areas). The strong and uniform signals at each location confirm even lignocaine distribution throughout the microneedle arrays. This level of spatial consistency is essential for maintaining predictable dosing in clinical applications, as irregular drug loading could result in underdosing or overdosing.

The confocal imaging results indicate a drug loading uniformity of ≥85%, providing clear visual confirmation that the formulation method produced consistent dispersion within the microneedle structure. The uniform distribution observed by CLSM reflects the importance of maintaining precision in microscale fabrication, similar to findings in microporous membrane studies for biological filtration [15], where uniform pore size directly affected both filtration performance and therapeutic reliability. In contrast to bulk quantification methods that infer homogeneity based on process alone, this optical approach directly verifies drug distribution at the microscale level [12]. This technique helps overcome a common limitation in microneedle research, where internal drug localization often remains unverified [14].

3.3. Nanoindentation

Figure 4 shows the nanoindentation load–displacement curves of maltose-based microneedles containing 0%, 25%, and 50% lignocaine. All tested samples showed distinct elastic recovery during the unloading phase, indicating that the microneedle structures tolerated compressive stress without sustaining permanent deformation. This resilience is critical to minimize tip breakage during insertion and ensure reliable skin penetration.

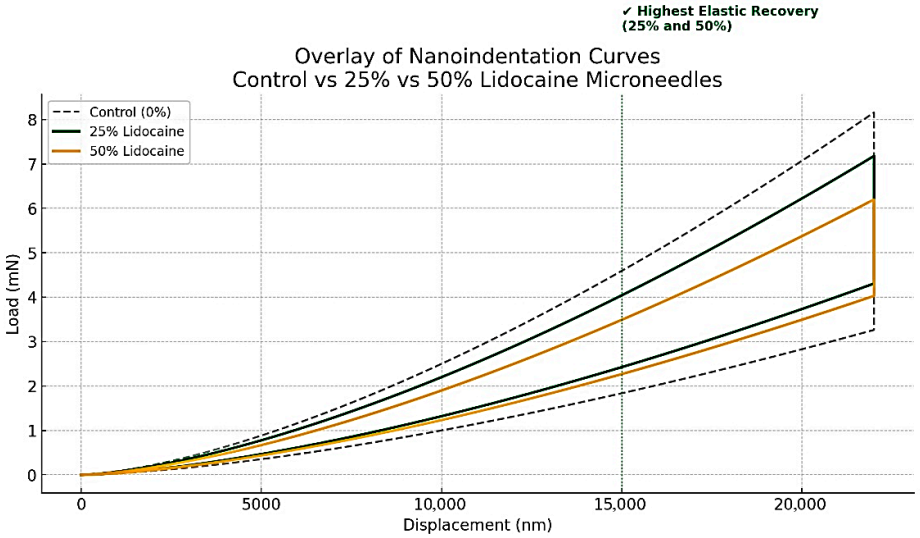

Figure 4. Nanoindentation Load–Displacement Curves Demonstrating Mechanical Strength and Elastic Recovery of Maltose-Based Lignocaine Microneedles at Three Lignocaine Concentrations.

The curves also show that microneedles containing lignocaine maintained mechanical strength comparable to or greater than that of the control group. Notably, the 25% and 50% lignocaine-loaded microneedles exhibited the highest levels of elastic recovery, indicating that drug incorporation did not weaken—and may have improved—the structural integrity of the maltose matrix. These results are consistent with earlier studies reporting that dissolvable microneedles can retain sufficient mechanical strength despite changes in composition [16]. The observed strength also meets the demands of lab-on-chip (LoC) systems [17], where microfabricated structures must endure localized pressure during fluid flow or membrane deformation [18].

These findings have important practical implications. Mechanically robust microneedles lower the risk of failure during use, which is particularly relevant in outpatient or self-administered settings where insertion force can vary among individuals. Additionally, the observed elastic recovery indicates that microneedles can penetrate the skin without fracturing, enhancing both user safety and confidence in application [18]. Recent evaluations of commercial microneedle patches also emphasize the need for strong mechanical properties to ensure reliable skin penetration performance in real-world applications [19].

Overall, the nanoindentation results confirm the feasibility of using maltose–lignocaine microneedles as a reliable transdermal delivery system. This platform combines several key advantages: a biocompatible sugar-based matrix, consistent geometric structure, and mechanical strength adequate for reliable skin insertion [20]. These features, along with the potential for rapid drug onset, underscore its potential benefits over conventional topical anesthetic formulations such as Eutectic Mixture of Local Anesthetics (EMLA) [19].

3.4. Comparison of Microneedle Fabrication Method with Previously Published Systems

Table 1 summarizes how the current fabrication method compares with prior dissolvable microneedle systems. Compared to other studies, our method uses a low-cost, single-step process without requiring backing films or complex layering. The mechanical strength and drug uniformity achieved are on par or better than those in earlier reports, supporting the practical value of this approach.

Table 1. Comparison of lignocaine/lidocaine microneedle systems and conventional topical anesthetics.

Study	Material	Drug	Fabrication Method	Mechanical Strength (N/Needle)	Drug Uniformity	Notable Features
This study	Maltose	Lignocaine	Micromolding	~0.6 N	≥85% (CLSM verified)	Simple, low-cost process; no backing layer
Jiang et al. (2023) [20]	Isomaltulose (ISO)	Lidocaine hydrochloride (LIDH)	3D-printing-supported mold microneedle casting	Up to ~80%	Not reported	High drug loading
Mao et al. (2023) [21]	PVP/PVA/HA (1:2:1)	Lidocaine hydrochloride	Micromolding	>0.1 N/needle	Visual but not quantified	Only confirms loading amount, not distribution uniformity
Loizidou et al. [22]	CMC/SUC, CMC/MAL, CMC/TRD	Propranolol	Vacuum mold casting	Up to 7.42 GPa (modulus)	Not assessed	CLSM used only for skin insertion
Jin et al. [23]	PVP/PVA	Lidocaine HCl	Double casting	0.32 N/needle	Quantified by HPLC only	OCT showed insertion, no CLSM

4. Conclusions

This study successfully demonstrated the fabrication and characterization of maltose-based dissolving microneedles (DMNs) loaded with lignocaine. SEM analysis showed reproducible microneedle dimensions with low variability and achieved uniform drug distribution across the matrix, validated via CLSM. Mechanical testing showed that each microneedle exceeded the minimum force required for effective skin penetration, while retaining elasticity and structural integrity. These results show structural stability, consistent

drug distribution as verified by CLSM, and adequate mechanical strength of the fabricated DMNs, which support their potential as a safe, painless alternative for localized anesthetic delivery. While further studies, such as Franz diffusion and in vitro dissolution testing, are currently ongoing, these findings support the feasibility of this platform as a safe, reproducible option for local anesthetic delivery.

Author Contributions: Conceptualization, A.A.H., A.G.I., and F.-C.C.; methodology, A.S.R. and M.E.A.N.; fabrication and investigation, A.S.R. and M.E.A.N.; optical characterization, A.S.R.; mechanical characterization, A.S.R., M.E.A.N. and A.A.H.; data analysis, A.S.R. and M.E.A.N.; resources, M.A.M., P.C.O., M.R.B., C.F.D., F.-C.C., M.-L.C.B., X.Y.C., C.L. and Y.Y.M.; writing—original draft preparation, A.S.R. and M.I.A.J.; writing—review and editing, A.G.I., A.A.H., M.I.A.J., C.S.G.; visualization, A.S.R.; supervision, A.G.I. and A.A.H.; project administration, A.G.I.; funding acquisition, A.G.I. and A.A.H. All authors have read and agreed to the published version of the manuscript.

Funding: This research is funded by the Fundamental Research Grant Scheme (FRGS/1/2023/STG07/UKM/02/5) research fund from the Ministry of Higher Education (MoHE), Malaysia.

Institutional Review Board Statement: Not applicable.

Informed Consent Statement: Not applicable.

Data Availability Statement: The data presented in this study are available from the corresponding authors upon reasonable request.

Acknowledgments: The authors would like to extend their sincere appreciation to the Institute of Microengineering and Nanoelectronics (IMEN), Department of Paediatrics, Department of Pharmacy at Hospital Canselor Tuanku Muhriz (HCTM) and Universiti Kebangsaan Malaysia (UKM) for providing technical support and access to research facilities. The contributions of all individuals and institutions involved have been instrumental to the successful completion of this study.

Conflicts of Interest: The authors declare no conflicts of interest. Dr. Chee Seong Goh has confirmed that Alnair Photonics Sdn Bhd has no commercial conflict of interest.

References

1. Barry, B.W. Novel mechanisms and devices to enable successful transdermal drug delivery. *Eur. J. Pharm. Sci.* **2001**, *14*, 101–114. [CrossRef] [PubMed]
2. Sartawi, Z.; Blackshields, C.; Faisal, W. Dissolving microneedles: Applications and growing therapeutic potential. *J. Control. Release* **2022**, *348*, 186–205. [CrossRef] [PubMed]
3. Larrañeta, E.; Lutton, R.E.M.; Woolfson, A.D.; Donnelly, R.F. Microneedle arrays as transdermal and intradermal drug delivery systems: Materials science, manufacture and commercial development. *Mater. Sci. Eng. R Rep.* **2016**, *104*, 1–32. [CrossRef]
4. Gordh, T.; Gordh, T.E.; Lindqvist, K.; Warner, D.S. Lidocaine: The Origin of a Modern Local Anesthetic. *Anesthesiology* **2010**, *113*, 1433–1437. [CrossRef] [PubMed]
5. Zhang, Y.; Jiang, G.; Yu, W.; Liu, D.; Xu, B. Microneedles fabricated from alginate and maltose for transdermal delivery of insulin on diabetic rats. *Mater. Sci. Eng. C* **2018**, *85*, 18–26. [CrossRef] [PubMed]
6. Rad, Z.F.; Prewett, P.D.; Davies, G.J. An overview of microneedle applications, materials, and fabrication methods. *Beilstein J. Nanotechnol* **2021**, *12*, 1034–1046. [CrossRef]
7. Peeni, B.A.; Lee, M.L.; Hawkins, A.R.; Woolley, A.T. Sacrificial layer microfluidic device fabrication methods. *Electrophoresis* **2006**, *27*, 4888–4895. [CrossRef] [PubMed]
8. Oliver, W.C.; Pharr, G.M. An improved technique for determining hardness and elastic modulus using load and displacement sensing indentation experiments. *J. Mater. Res.* **1992**, *7*, 1564–1583. [CrossRef]
9. Wang, Q.L.; Ren, J.W.; Chen, B.Z.; Jin, X.; Zhang, C.Y.; Guo, X.D. Effect of humidity on mechanical properties of dissolving microneedles for transdermal drug delivery. *J. Ind. Eng. Chem.* **2018**, *59*, 251–258. [CrossRef]
10. Hamzah, A.A.; Majlis, Y.; Ahmad, I. Deflection Analysis of Epitaxially Deposited Polysilicon Encapsulation for MEMS Devices. In Proceedings of the 2004 IEEE International Conference on Semiconductor Electronics, Kuala Lumpur, Malaysia, 7–9 December 2004.
11. Faraji Rad, Z.; Prewett, P.D.; Davies, G.J. Rapid prototyping and customizable microneedle design: Ultra-sharp microneedle fabrication using two-photon polymerization and low-cost micromolding techniques. *Manuf. Lett.* **2021**, *30*, 39–43. [CrossRef]

12. Wang, Q.L.; Zhu, D.D.; Chen, Y.; Guo, X.D. A fabrication method of microneedle molds with controlled microstructures. *Mater. Sci. Eng. C* **2016**, *65*, 135–142. [CrossRef] [PubMed]
13. Monou, P.K.; Saropoulou, E.; Junqueira, L.A.; Kolipaka, S.S.; Andriotis, E.G.; Tzimtzimis, E.; Tzetzis, D.; Bekiari, C.; Bouropoulos, N.; Harding, B.; et al. Fabrication and characterization of dissolving microneedles combining digital light processing and vacuum compression molding technique for the transdermal delivery of rivastigmine. *Eur. J. Pharm. Biopharm.* **2025**, *210*, 114687. [CrossRef] [PubMed]
14. Park, J.H.; Allen, M.G.; Prausnitz, M.R. Polymer microneedles for controlled-release drug delivery. *Pharm. Res.* **2006**, *23*, 1008–1019. [CrossRef] [PubMed]
15. Hamzah, A.A.; Zainal Abidin, H.E.; Yeop Majlis, B.; Mohd Nor, M.; Ismardi, A.; Sugandi, G.; Tiong, T.Y.; Dee, C.F.; Yunas, J. Electrochemically deposited and etched membranes with precisely sized micropores for biological fluids microfiltration. *J. Micromechanics Microengineering* **2013**, *23*, 074007. [CrossRef]
16. Ando, D.; Miyatsuji, M.; Sakoda, H.; Yamamoto, E.; Miyazaki, T.; Koide, T.; Sato, Y.; Izutsu, K.I. Mechanical Characterization of Dissolving Microneedles: Factors Affecting Physical Strength of Needles. *Pharmaceutics* **2024**, *16*, 200. [CrossRef] [PubMed]
17. Aziz, N.A.; Bais, B.; Hamzah, A.A.; Majlis, B.Y. Characterization of HNA etchant for silicon microneedles array fabrication. In Proceedings of the 2008 IEEE International Conference on Semiconductor Electronics, Johor Bahru, Malaysia, 25–27 November 2008.
18. Marsi, N.; Majlis, B.Y.; Hamzah, A.A.; Mohd-Yasin, F. Comparison of mechanical deflection and maximum stress of 3C SiC- and si-based pressure sensor diaphragms for extreme environment. In Proceedings of the 2012 10th IEEE International Conference on Semiconductor Electronics (ICSE), Kuala Lumpur, Malaysia, 19–21 September 2012; pp. 186–190.
19. Kochhar, J.S.; Lim, W.X.S.; Zou, S.; Foo, W.Y.; Pan, J.; Kang, L. Microneedle integrated transdermal patch for fast onset and sustained delivery of lidocaine. *Mol. Pharm.* **2013**, *10*, 4272–4280. [CrossRef] [PubMed]
20. Jiang, X.; Wang, S.; Zhang, L.; Jiang, X.; Gou, M. Lidocaine hydrochloride loaded isomaltulose microneedles for efficient local anesthesia of the skin. *Chin. Chem. Lett.* **2024**, *35*, 108686. [CrossRef]
21. Mao, Y.; Zhang, X.; Sun, Y.; Shen, Z.; Zhong, C.; Nie, L.; Shavandi, A.; Yunusov, K.E.; Jiang, G. Fabrication of lidocaine-loaded polymer dissolving microneedles for rapid and prolonged local anesthesia. *Biomed. Microdevices* **2024**, *26*, 9. [CrossRef] [PubMed]
22. Loizidou, E.Z.; Williams, N.A.; Barrow, D.A.; Eaton, M.J.; Mccrory, J.; Evans, S.L.; Allender, C.J. Structural characterisation and transdermal delivery studies on sugar microneedles: Experimental and finite element modelling analyses. *Eur. J. Pharm. Biopharm.* **2015**, *89*, 224–231. [CrossRef] [PubMed]
23. Jin, S.Y.; Park, E.J.; Kwon, S.M.; Jung, H.; Kim, D.W. Rapidly Dissolving Microneedles Incorporating Lidocaine Hydrochloride: A PVP/PVA-Based Approach for Local Anesthesia. *Pharmaceutics* **2025**, *17*, 1100. [CrossRef] [PubMed]

Disclaimer/Publisher's Note: The statements, opinions and data contained in all publications are solely those of the individual author(s) and contributor(s) and not of MDPI and/or the editor(s). MDPI and/or the editor(s) disclaim responsibility for any injury to people or property resulting from any ideas, methods, instructions or products referred to in the content.